

## Analysis and compensation of the reflector antenna pointing error under wind disturbance

Qian Xu<sup>1,2</sup>, Jie Zhang<sup>1,3</sup>, Zhao-Yu Wang<sup>3</sup> and Huan-Zhi Pan<sup>3</sup>

<sup>1</sup> Xinjiang Astronomical Observatory, Chinese Academy of Sciences, Urumqi 830011, China; [xuqian@xao.ac.cn](mailto:xuqian@xao.ac.cn)

<sup>2</sup> Key Laboratory of Chinese Academy of Sciences for Radio Astronomy, Urumqi 830011, China

<sup>3</sup> Xidian University, Key Laboratory of Electronic Equipment Structure Design, Ministry of Education, Xi'an 710071, China

Received 2020 August 31; accepted 2021 January 27

**Abstract** A large reflector antenna has been widely used in satellite communications, gravitational wave detection, galaxy origin observation and other fields due to its narrow beam and high gain. With the increase of the antenna aperture and the improvement of the working frequency, the requirements for the pointing accuracy of an antenna are also rising. However, the effect of environmental load on the deformation of the antenna structure, which in turn affects its beam pointing, has become a key problem to be solved urgently in the antenna engineering applications. The key issue to solving this problem involves accurately estimating the pointing error caused by the structural deformation and designing an effective controller that is based on the structural deformation. In this paper, we first establish a dynamic model for antenna structure based on the modal superposition method. The model is then modified by using modal characteristics and the dynamic displacement information of the sampling points to achieve the purpose of accurately estimating the structural deformation. Secondly, by considering the influence of the deformation of the rotating shaft and the reflector surface on the pointing accuracy, a control-oriented pointing error analysis model is established for estimating the pointing error caused by the environmental load in real time. Thirdly, based on considering the influence of the shaft deformation on the error compensation, the feedback error amount is decoupled and corrected to improve the accuracy of the compensation error. Finally, this paper analyzes and verifies the 65 m S/X-band dual reflector antenna with a numerical example. We consider a fluctuating wind with an average wind speed of  $10 \text{ m s}^{-1}$  as an example, which results in a maximum pointing error of  $55.82''$  as calculated by the antenna theoretical model, whereas the maximum pointing error as predicted by our model is  $68.27''$ . The pointing error after compensating for the cause of the environmental load with the modified controller is reduced to  $10.57''$ , which effectively improves the antenna pointing performance.

**Key words:** telescopes — methods: analytical — methods: numerical

### 1 INTRODUCTION

In practical engineering, the pointing accuracy refers to the closeness of pointing from an antenna beam to the predetermined pointing at a certain elevation angle after taking into account various errors and deformations. It indicates the accuracy of the antenna system in target pointing. It also reflects the ability of an antenna in adjusting for the pointing direction based on received instructions and tracking the moving target in real time, which is an important indicator in the antenna system (Zhang et al. 2018). QiTai radio Telescope (QTT) (Wang 2014) is a 110 m diameter and fully steerable radio

telescope, which will be built in the Qitai County of Xinjiang in China. The requirement of the telescope for pointing is less than  $2.5''$ . As it operates in open air, the environment loads will have significant impact on the pointing accuracy of the telescope (He et al. 2020).

Accurately estimating the pointing error caused by environmental loads is the key to compensating the pointing error caused by the latter. In the study of the antenna base shaft system, the influence of the shaft system on pointing accuracy is divided into three scenarios. They can be described as the pitch axis and the azimuth axis being not orthogonal to each other, the azimuth axis being not vertical, and the electrical axis and the pitch

axis being not vertical, and error analysis for each is performed separately (Liu et al. 2018). In order to reduce the influence of the three shafting errors on the pointing accuracy, the common control and adjustment methods in engineering practice are introduced in detail (Gu & Zhao 2017). Zhang et al. divided the pointing error caused by the deformation of the reflector into four aspects, which are the lateral displacement of the feed, the rotation of the feed, the deformation of the reflector surface, and the rotation of the sub-reflector. Then, the coupling effect of various aspects was considered comprehensively to establish the pointing error estimation model (Zhang et al. 2016).

In the models for estimating the pointing errors mentioned above, most of them consider only the antenna base axis error or the reflector error. However, ignoring the antenna pointing accuracy is the result of the joint effect of the antenna base axis error and the reflector deformation, which leads to precision limitations. The pointing error analysis model for control is often based on modal superposition method and the approximate optical method, but this method depends on the accuracy of the error model, and the estimated pointing accuracy often has a large error (Yu & Fan 2019).

The current research on pointing errors caused by slowly changing loads, such as in the temperature and gravity, is relatively mature. According to the matching relationship between the main reflector and the sub-reflector, the position of the sub-reflector at each elevation angle of the antenna is calculated and the position of the sub-reflector is adjusted in real time by referring to the table to compensate for the deformation of the main reflector caused by gravity (Leng et al. 2018). According to the requirements for the antenna beam pointing, a calculation method is proposed for panel adjustment of the deformed parabolic antenna facing gain and pointing. The method is based on the best fitting paraboloid as the reference surface combining with the minimization of the actuator stroke. Through the panel adjustment, the pointing deviation caused by the antenna structure deformation is compensated for (Wang et al. 2017). By using photogrammetry technology, the deformation of the antenna reflector surface of the 22m antenna at different elevation angles is obtained, and the influence on the antenna pointing electrical performance is analyzed (Subrahmanyam 2005). The multi-body system theory is used to establish the transfer function relationship between geometric errors and pointing errors. After the pointing error model is established, the model parameters are corrected through the pointing error obtained from experimental data. The experiment shows that the accuracy of the model after correction is increased by about 8%,

which can correct most of the system errors related to the pointing error (Huang et al. 2016).

Due to its good repeatability, the environment loads characterized by slow changes in temperature and gravity can be compensated satisfactorily. However, owing to its transient properties and randomness, wind disturbance has become the main factor that restricts the pointing accuracy of an antenna. The influence of wind disturbance on the antenna pointing can be categorized into three types, namely the wind acting on the antenna reflector surface, the torque disturbance acting on the antenna motor shaft and the speed disturbance acting on the input of the speed loop (Gawronski 2004). We analyze the average wind load response of the antenna structure under different windward attitudes and different wind speeds, as well as the variation of antenna surface shape accuracy and pointing accuracy. The results show that the average wind load has a great impact on the antenna pointing accuracy, especially on the elevation angle pointing accuracy, but has a small effect on the surface shape accuracy. We find that the antenna surface shape accuracy and pointing accuracy have a quadratic relationship with the wind speed within the elastic range (Li et al. 2019). The autoregressive filtering method is used to simulate the random process of gusts by treating the gust effect as a torque that changes with time. The model is then applied to a typical 34 m Cassegrain antenna servo system, and the results of simulation are highly consistent with that obtained from site measurement (He et al. 2009). The pointing error caused by the structural deformation is also analyzed, and an antenna model for the pointing control of flexible deformation of the structure is proposed. In addition, a linear quadratic Gaussian controller is designed to suppress wind disturbance (Zhang et al. 2015).

In the above compensation for the pointing error caused by the environmental load, either the controller feedback signal is taken as the only rigid angle of the antenna, or the pointing compensation is performed by adjusting the shape of the reflector, or the pointing error caused by the wind is not estimated. Even though the pointing error caused by the deformation of the reflector is estimated and introduced in the feedback, it has certain limitations due to the omission of the influence of the shaft deformation on the pointing error and the independent compensation method of the pitch and azimuth directions.

This paper revises the pointing error estimation method and the control compensation method for the pointing error, respectively. By weighting and correcting the antenna dynamic model, a pointing error analysis model is established which takes into account the deformation of the shaft and the reflector comprehensively and introduces the influence of the shaft deformation on

the pointing accuracy into the controller. The goal of improving the pointing accuracy of the reflector antenna is finally achieved.

## 2 APPROXIMATE DYNAMIC MODEL OF ANTENNA

A large aperture antenna is mainly composed of a reflector, pitching bracket and azimuth turntable. Deformation of any part of the antenna will lead to deflection of the antenna. Therefore, obtaining the deformation information of each antenna structure under environmental load is the basis and premise of analyzing the pointing error caused by the environmental load.

The dynamic model of the antenna structure in generalized coordinates can be expressed as follows:

$$M\ddot{q} + D\dot{q} + Kq = B_0u, \quad (1)$$

$$y = C_{0q}q, \quad (2)$$

where the diagonal matrixes,  $M$ ,  $D$ , and  $K$ , are the mass matrix, damping matrix and stiffness matrix respectively. Here,  $B_0$  and  $C_{0q}$  are the input matrix and the output matrix, respectively,  $q$  is the node displacement vector,  $u$  is the input load, and  $y$  is the output node displacement.

In order to decouple the equations, the modal displacement  $q_m$  and the mode matrix  $\Phi$  are introduced. They satisfy the following equations:

$$q = \Phi q_m, \quad (3)$$

$$\Phi = \begin{bmatrix} \varphi_{11} & \varphi_{21} & \cdots & \varphi_{n1} \\ \varphi_{12} & \varphi_{22} & \cdots & \varphi_{n2} \\ \cdots & \cdots & \cdots & \cdots \\ \varphi_{1k} & \varphi_{2k} & \cdots & \varphi_{nk} \\ \cdots & \cdots & \varphi_{ij} & \cdots \\ \varphi_{1n_d} & \varphi_{2n_d} & \cdots & \varphi_{nn_d} \end{bmatrix}, \quad (4)$$

where  $\varphi_{ij}$  is the displacement of the  $j$ th degree of freedom in the  $i$ th mode.

Substituting (3) into (1) and multiplying  $\Phi^T$  from left, the dynamic equation based on absolute coordinates is transformed into a dynamic equation based on modal coordinates:

$$M_m\ddot{q}_m + D_m\dot{q}_m + K_mq_m = \Phi^T B_0u, \quad (5)$$

$$y = C_{0q}\Phi q_m. \quad (6)$$

The model selects the node displacement  $q_m$  in the modal coordinate system as the state variable and takes various environmental loads as inputs, while treating the displacement  $y$  of each node in the natural coordinate system as the output. The displacement output can reflect the deformation of the antenna structure and is used to

estimate the pointing error caused by the deformation of the antenna structure.

The  $M_m$ ,  $D_m$ ,  $K_m$  are, respectively, the modal mass matrix, the modal damping matrix and the modal stiffness matrix, and they can be obtained by modal analysis of the finite element model of the antenna structure.

Although the antenna deformation estimated by the dynamic model is closer to the actual deformation, there are still gaps between simulation and the actual deformation due to the complexity of the antenna structure and the limitations of the simulation software. With the increasing requirements for antenna pointing accuracy, it is necessary to modify the dynamic model of the antenna. The modified general idea is shown in Figure 1.

According to the dynamic model, the displacement of each node is obtained by the superposition of each mode shape, and is given by

$$X_l = \sum_{i=1}^n \Phi_{li} q_{mi}, \quad (7)$$

where  $X_l$  is the displacement of the  $l$ th degree of freedom,  $\Phi_{li}$  is an element in the  $l$ th row and  $i$ th column of the vibration mode matrix, and  $q_{mi}$  is the  $i$ th modal coordinate.

Let  $\alpha_i$  be the correction weight for the  $i$ th mode, the displacement of the degree of freedom after modal correction is

$$X_l = \sum_{i=1}^n \Phi_{li} (1 + \alpha_i) q_{mi}. \quad (8)$$

When the measured displacement  $X'_l$  for each node is known, the modal correction coefficient  $\alpha_i$  can be optimized using the measured deformation of the node. That is, the trust region algorithm is used to solve the weight coefficient  $\alpha_i$ , which can then be used to minimize the total error function  $S(\alpha) = \sqrt{\frac{\sum_{i=1}^n (X_i - X'_i)^2}{n}}$ . The optimization algorithm is shown in Figure 2. First, the initial iteration point  $\alpha_k$  and trust region radius  $\Delta_k$  are set, then the objective function  $S(\alpha)$  is expanded at the current iteration point to obtain the quadratic approximation model  $Q_k$ . It then followed by judging the accuracy of the approximate model based on  $r_k$  (the ratio of the original model's descent amount to the approximate model's descent amount). For  $r_k$  close to 1, the approximation model is successfully approached and the next iteration point  $\alpha_{k+1}$  is obtained. Otherwise, the trust region radius is reduced and the judgment continues. When the reduction of the original model is finally less than the predetermined threshold, the weight  $\alpha$  coefficient that minimizes the total error is obtained.

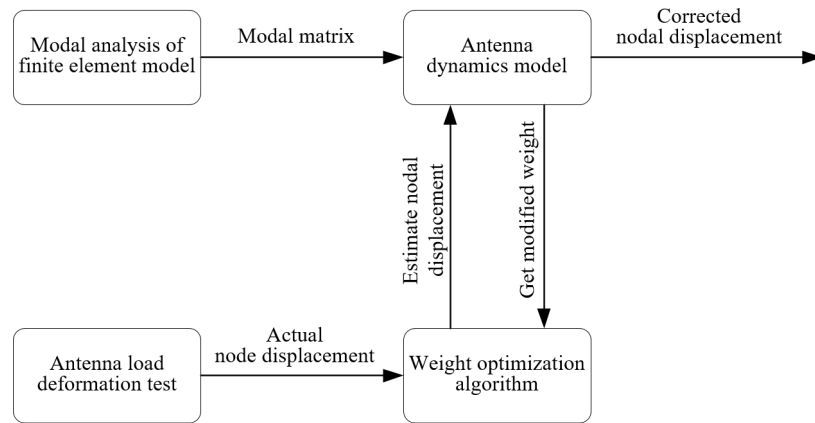


Fig. 1 Correction flowchart.

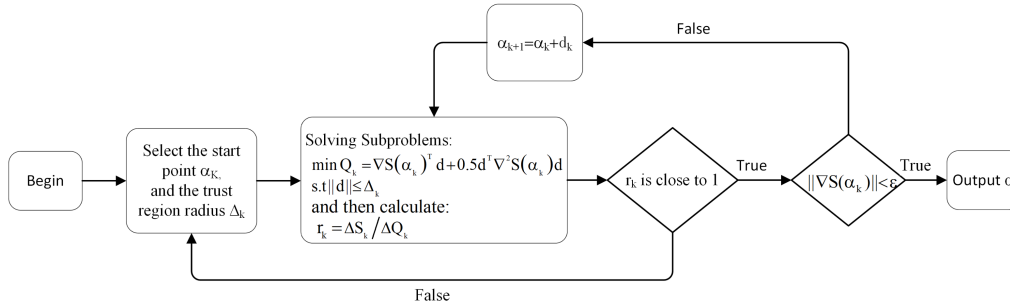


Fig. 2 Optimization algorithm flowchart.

### 3 ESTIMATION OF POINTING ERROR CAUSED BY STRUCTURAL DEFORMATION

For the reflector antenna, the main factors affecting its pointing performance include the deformation of the reflector, the azimuth axis and pitch axis. The deformation of the reflector (surface, feed and sub-reflector) will cause the electrical axis of the antenna to shift. The deformation of the antenna base (the pitch axis and azimuth axis) will cause the reflector, which connects to the base, to shift, thus affecting the pointing. The deformation of the reflector and the deformation of the antenna base are coupled with each other, and jointly affect the final pointing of the antenna.

In order to accurately describe the deformation of each axis of the antenna, and to study the relationship between the deformation of the antenna structure and the pointing accuracy, it is necessary to establish a reasonable coordinate system. This paper establishes three coordinate systems, as shown in Figure 3.

The geodetic coordinate system (absolute coordinate system), signified by  $OXYZ$ , is a coordinate system that has its origin at the center of the azimuth track. The  $Z$  axis

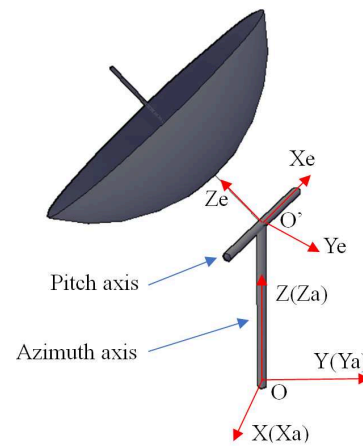


Fig. 3 Antenna coordinate system.

is perpendicular to the ground, and the negative direction of the  $Y$  axis points to the north direction.

The coordinate system represented by  $OX_aY_aZ_a$  is fixed to the azimuth axis with the origin located at the center of the azimuth track. The  $Z$  axis coincides with the azimuth axis, and the overall coordinate system moves with the rotation and deflection of the azimuth axis.

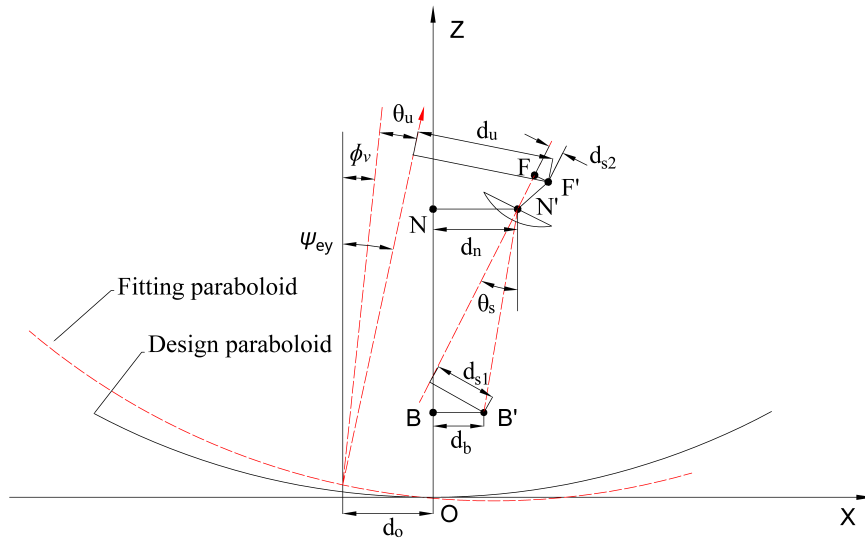


Fig. 4 Pointing error caused by the deformation of the reflective surface.

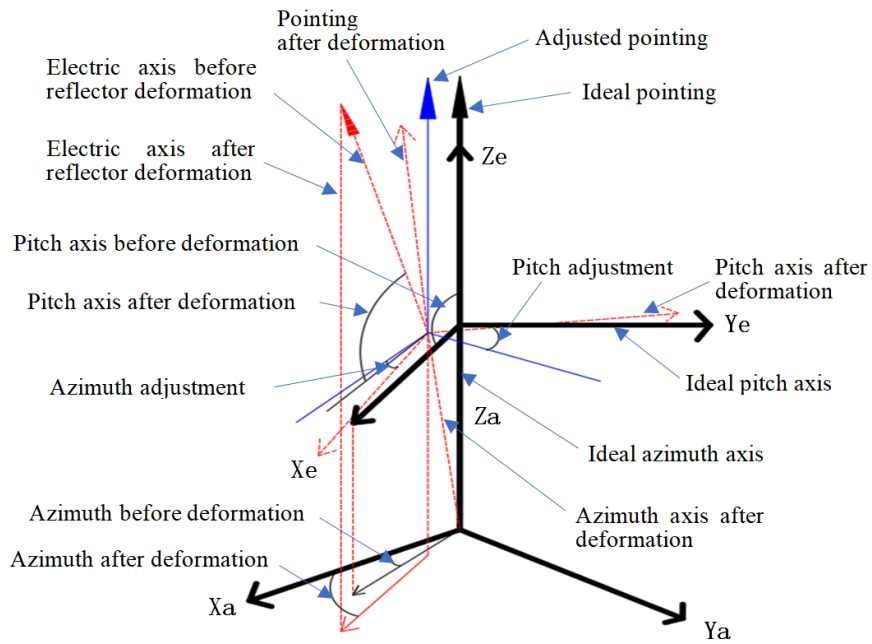


Fig. 5 Schematic diagram of compensation calculation.

The  $OX_eY_eZ_e$  is a coordinate system that is fixed to the pitch axis. The origin of the system is located at the midpoint of the pitch axis with the  $X$  axis coinciding with the pitch axis, and the overall coordinate system follows the rotation and deflection of the pitch axis. (When there is no axis error and the current azimuth angle of the antenna is 0, this coordinate system coincides with the geodetic coordinate system  $OXYZ$ .)

Based on the above three coordinate systems, the direction vector of the electric axis (the direction of the antenna electromagnetic wave) is transformed from the pitch axis coordinate system to the absolute coordinate system through coordinate transformation. The direction vector of the electric axis in the absolute coordinate system is deformed, and is compared with the direction vector in the ideal situation, which can be used to obtain the pointing error caused by the structural deformation.

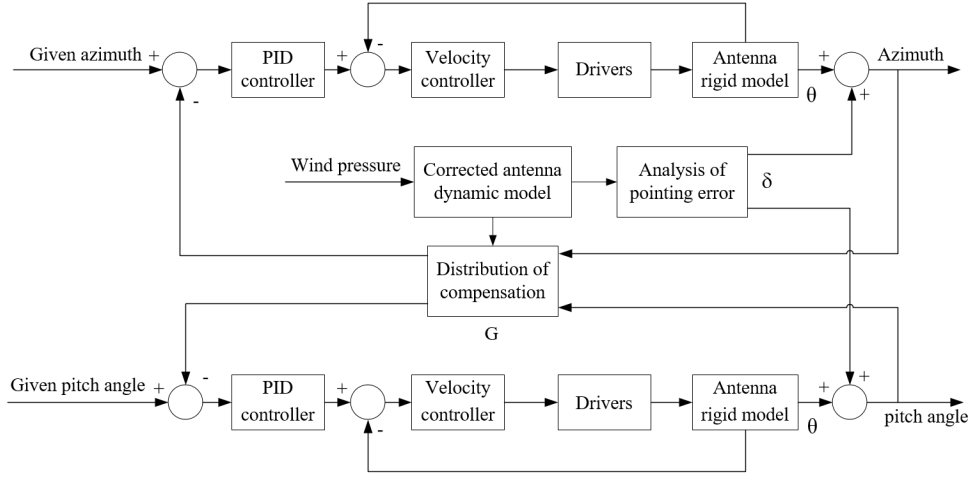


Fig. 6 Control block diagram for pointing error compensation.

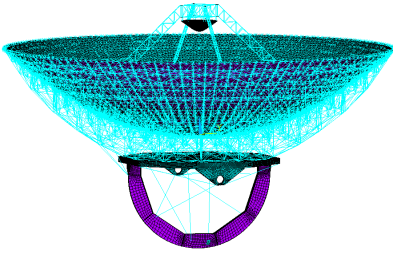


Fig. 7 65 m antenna finite element model.

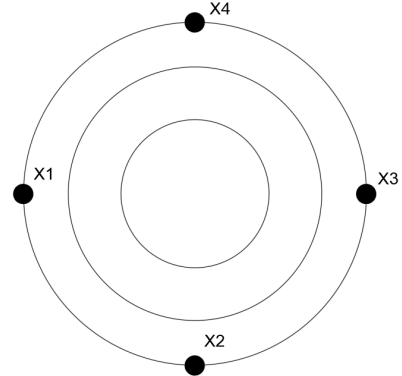


Fig. 8 Distribution of sampling points.

3.1 The Direction Vector of the Electric Axis in the Ideal Case

In the ideal case, in which neither the axis systems nor the reflector is deformed, the transformation matrix from the pitch axis coordinate system to the absolute coordinate system is

$$T = M(0, 0, -h)R_z(A)R_x\left(\frac{\pi}{2} - E\right), \quad (9)$$

where  $A$  is the azimuth angle of the antenna,  $E$  is the elevation angle of the antenna,  $M$  is the translation coordinate transformation matrix, and  $R$  is the rotation coordinate transformation matrix.

Ideally, the electrical axis direction vector in the pitch axis coordinate system is  $(0,0,1)$ , and the electrical axis direction vector in the absolute coordinate system is given by:

$$P = T * (0, 0, 1)^T = [\sin A \cos E - \cos A \cos E \sin E]^T. \quad (10)$$

3.2 The Direction Vector of the Electric Axis After Structure Deformation

Figure 4 shows the schematic diagram of pointing error caused by the deformation of the reflective surface. When the reflector is deformed under the environmental load and the displacement of the feed moves laterally, the rotation angle of the sub-reflector and the lateral displacement of the sub-reflector are expressed by  $d_b$ ,  $\theta_s$ , and  $d_n$ , respectively, and the vertex offset of the best fitting paraboloid along the  $w$ -axis and the rotation angle of the focal axis around the  $v$ -axis are denoted by  $d_o$  and  $\phi_v$  respectively. The error of the electric axis in the  $X_eZ_e$  plane and  $Y_eZ_e$  plane caused by the reflector deformation can be obtained by the following formulas (Zhang et al. 2018):

$$d_{s2} = \frac{L_3 \cos \theta_s |d_b + d_n + L_1 \tan \theta_s|}{L_1}, \quad (11)$$

$$\psi_{ey} = \frac{-|\tan\phi_v(L_1 + L_3 \cos\theta_s - d_{s2} \sin\theta_s) - (d_n + L_3 \sin\theta_s + d_{s2} \cos\theta_s) + \tan\phi_v L_2 - d_0|k}{\sqrt{1 + (\tan\phi_v)^2}f} + \phi_v \quad (12)$$

Here,  $L_1$  is the distance from the feed B to the center point N of the sub-reflector,  $L_2$  is the distance from the feed B to the center point O of the main reflector,  $L_3$  is the distance from the focal point F of the sub-reflector to the center N' of the sub-reflector, and K is the beam deflection factor.

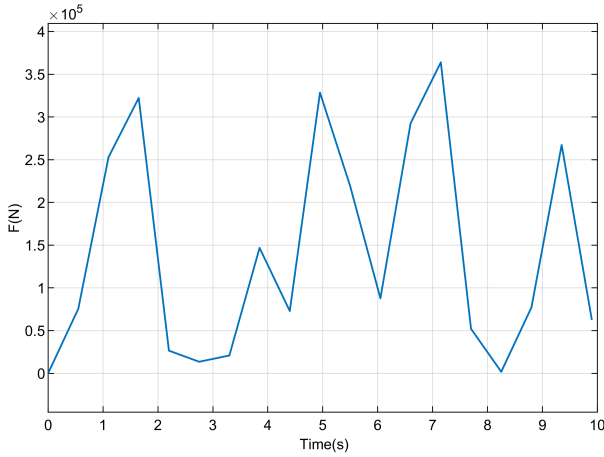


Fig.9 Wind input.

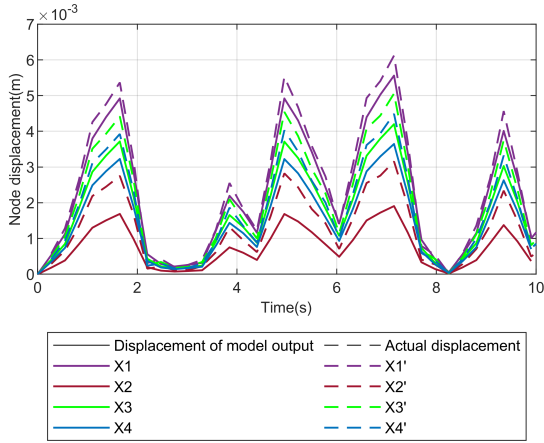


Fig.10 Comparison diagram of node displacement and actual displacement before correction.

Assume that the electric axis deviation caused by the deformation of the reflector in the  $X_e Z_e$  and  $Y_e Z_e$  planes of the pitching coordinate system is represented by  $\psi_{ex}$ ,  $\psi_{ey}$ , the direction vector of the electric axis in the pitching coordinate system becomes  $(\tan\psi_{ex}, \tan\psi_{ey}, 1)$ .

Under the influence of environmental load, the pitch axis and azimuth axis of the antenna also deform, and the transformation matrix  $T'$  from the pitching coordinate

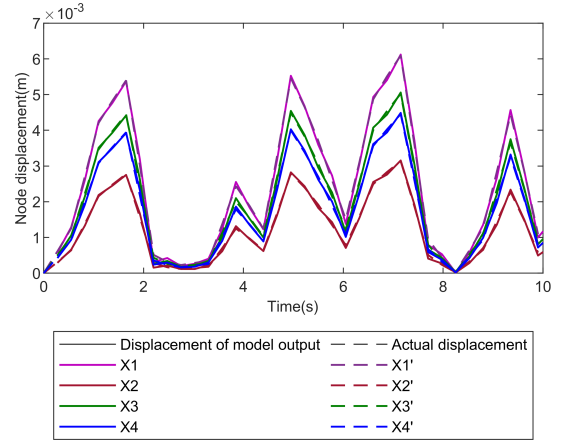


Fig.11 Comparison of the corrected model output displacement and the actual displacement.

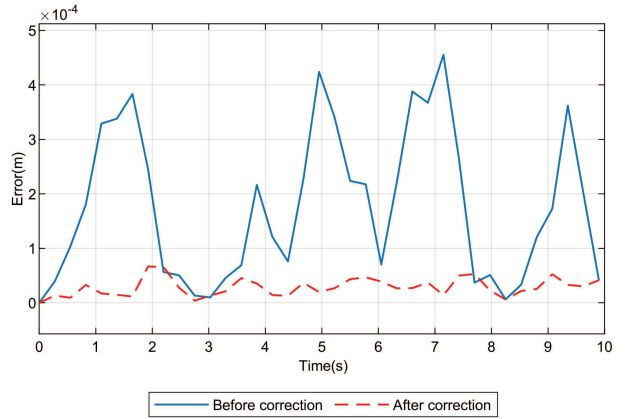


Fig.12 Error analysis before and after dynamic model correction.

system to the absolute coordinate system becomes

$$T' = M(0, 0, -h)R_y(\varphi_{ay})R_x(\varphi_{ax})R_z(A) \times R_z(\varphi_{ez})R_y(\varphi_{ey})R_x\left(\frac{\pi}{2} - E\right), \quad (13)$$

where  $\varphi_{ax}$ ,  $\varphi_{ay}$  are the angular displacement error of the azimuth axis around the  $X_a, Y_a$  axes respectively, and  $\varphi_{ey}$ ,  $\varphi_{ez}$  are the angular displacement errors of the pitch axis around the  $Y_e, Z_e$  axes, respectively.

Then the coordinates of the electrical axis direction vector in the absolute coordinate system after the antenna structure is deformed can be obtained from:

$$P' = T' * (\tan \psi_{ex}, \tan \psi_{ey}, 1)^T. \quad (14)$$

### 3.3 Pointing Error Estimation

By comparing the direction vectors  $P$  and  $P'$  of the electrical axis in the absolute coordinate system before and after the deformation, the total pointing error when the reflector, the azimuth axis, and pitch axis are simultaneously deformed can be obtained from:

$$\delta = \cos^{-1}\left(\frac{P * P'}{|P| * |P'|}\right). \quad (15)$$

The projections  $\alpha$  and  $\beta$  in the azimuth direction and the pitch direction are, respectively, given by

$$\alpha = \tan^{-1}\left(\frac{P'(1)}{P'(2)}\right) - A, \quad (16)$$

$$\beta = \tan^{-1}\left(\frac{P'(3)}{\sqrt{P'(1)^2 + P'(2)^2}}\right) - E. \quad (17)$$

## 4 CONTROLLER DESIGN

Based on the relative independence of the servo system in the pitch direction and in the azimuth direction, the traditional control algorithm for pointing compensation for flexible antenna structures usually decouples the pointing error into the pointing error in the pitch direction and the pointing error in the azimuth direction. It then takes the minimum error of the two directions as the target, and compensates by the respective servo control system. This method can effectively compensate the error caused by the deformation of the reflector.

However, when considering the influence of the shaft on the pointing error, the compensation effect of this method is not ideal. Therefore, this paper proposes a method to combine the azimuth and the pitch directions with the aim to minimize the total pointing error and to achieve the goal of accurately compensating the pointing error by reasonably allocating the respective adjustment amount. Figure 5 shows the compensation calculation.

Let  $\Delta A$  and  $\Delta E$  be the adjustment amount of azimuth and elevation, respectively, then Equation (13) for the transformation matrix from the pitching coordinate system to the absolute coordinate system becomes:

$$T'' = M(0, 0, -h)R_y(\varphi_{ay})R_x(\varphi_{ax})R_z(\Delta A + A) \\ \times R_z(\varphi_{ez})R_y(\varphi_{ey})R_x\left(\frac{\pi}{2} - E - \Delta E\right). \quad (18)$$

From Equation (14), the adjusted pointing is

$$P'' = T'' * (\tan \psi_{ex}, \tan \psi_{ey}, 1)^T, \quad (19)$$

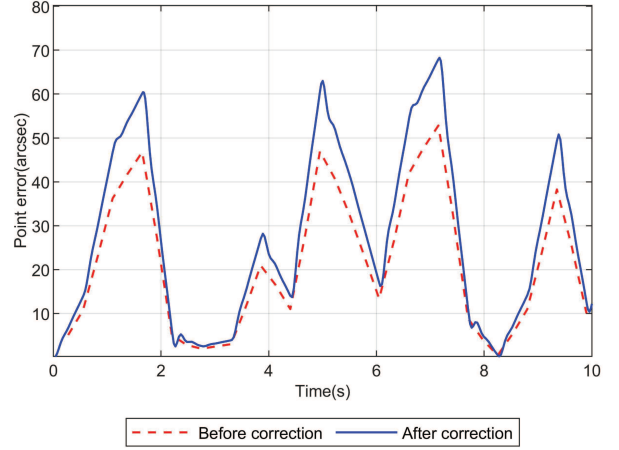


**Fig. 13** Comparison diagram of the estimated pointing error before and after correction.

and making the adjusted total pointing deviation minimum, we have

$$\delta = \cos^{-1}\left(\frac{P * P''}{|P| * |P''|}\right) = 0. \quad (20)$$

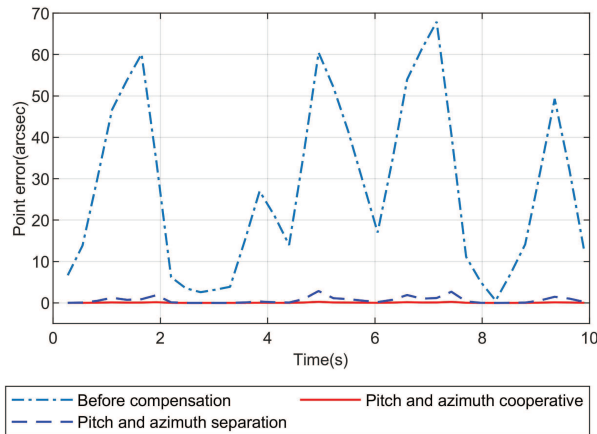
By solving the above two nonlinear equations and assuming minimum total pointing, the adjustment amount in the pitching direction and in the azimuth direction can be obtained.

Figure 6 shows the design of the controller block in this paper, which is based on the above correction for the compensation calculation incorporating the shaft deformation. Firstly, the displacement of each node is obtained from the modified antenna dynamic model, and then the pointing error  $\delta$  of the antenna under the environmental load is obtained from the pointing error estimation model according to the displacement of each node. Secondly, based on the estimated  $\delta$ , the deformation of the rotation axis and the current position of the antenna, the compensation amount for each direction is calculated using the compensation amount allocation module G through Formula 20. Finally, the calculated compensation amount  $\Delta A$ ,  $\Delta E$  is used as the feedback of the rotation angle error, then passing through the PID (Proportional Integral Derivative) controller, the direction is compensated.

## 5 ANALYTICAL EXAMPLES

### 5.1 Verification of the Correction Effect in the Dynamic Model

We assume an antenna with a diameter of 65 m as an example, as shown in Figure 7, and select four sampling points based on the principle that the deformation of the previous two-order mode is the largest. Figure 8 shows the approximate distribution of the sampling points.



**Fig. 14** Comparison diagram for the accuracy of compensation calculation.

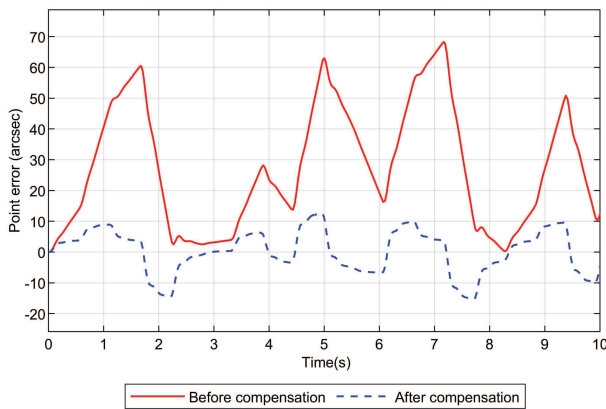


**Fig. 15** Comparison diagram before and after pointing error control compensation.

Under the effect of the random disturbance shown in Figure 9, the comparison of the node displacement output from the dynamic model and the actual node displacement is made, which is shown in Figure 10.

According to the results, we find that the output of the dynamic model is generally in line with the actual situation, but large errors still remain. Figure 11 shows the output displacement and actual displacement of each sampling point model after weighting and correcting for each mode. By comparing the root-mean-square error of the sampling point model before and after the correction, as shown in Figure 12, we can see that the maximum error predicted by the modified dynamic model in this paper is reduced from 4.5 mm to 0.6671 mm, which improves the accuracy of the dynamic model.

The comparison of the pointing error estimation using the deformation information output from the dynamic model before and after correction is shown in Figure 13. Applying the pointing error analysis model described in this paper to the output of the traditional dynamic model

as the measured deformation information, we estimate that the maximum pointing error is 55.82". If the model error is considered and the dynamic model is corrected by the correction method proposed in this paper, the maximum pointing error is estimated to be 68.27" with the corrected node deformation information.

## 5.2 Verification of the Control Compensation Effect

In order to verify the correctness of the compensation calculation in this paper, we consider an example using the 65 m antenna with an elevation angle of  $\pi/4$  and azimuth angle of 0. Under the random wind load of  $10 \text{ m s}^{-1}$  and without considering the inertial delay of the control system, the compensation amount of pitching and azimuth is directly added to calculate the compensated pointing error. Figure 14 shows the comparison diagram of the traditional pitch and azimuth independent compensation and the pitch and azimuth coordinated compensation proposed in this paper. It can be seen from the figure that the maximum error caused by structural deformation is 68.27" and the maximum residual error after compensation calculated using the traditional methods is 2.867", whereas the residual maximum pointing error using our model is only 0.2606". It is clear that the compensation calculated in this paper is more accurate.

Figure 15 shows the pointing performance of the antenna servo system with the PID controller under certain environmental loads. Before compensating the pointing error caused by wind, the maximum pointing error can reach 68.27". However, after introducing the pointing error estimation  $\delta$  and the compensation allocation module  $G$  into the position loop controller, the maximum pointing error is 10.57" and its root-mean-square error is only 5.07".

## 6 CONCLUSIONS

The elastic deformation of large reflector antennas has an increasingly significant impact on pointing accuracy. The traditional pointing error estimation methods either ignore the coupling effect of the reflector deformation and shaft deformation, or omit the modeling error of the dynamic model. To resolve these problems, this paper proposes a pointing error analysis method, based on coordinate transformation, and a dynamic model modification method using modal weighting. The results of simulation, assuming a 65 m antenna, show that our methods can accurately estimate the pointing error caused by the deformation of the large reflector antenna structure. In addition, the pointing performance of the antenna is improved after the error is compensated.

**Acknowledgements** This work was supported by the Chinese Academy of Sciences (CAS) “Light of West China” Program (No. 2017-XBQNXZ-B-023), the Xinjiang Uygur Autonomous Region “Tianshan innovation team” (No. 2018D14008), the Heaven lake Hundred-Talent Program of Xinjiang Uygur Autonomous Region of China 2017, the Natural Science Basic Research Plan in Shaanxi province of China (No. 2019JQ-269) and the Operation, Maintenance and upgrading Fund for Astronomical Telescopes and Facility Instruments, budgeted from the Ministry of Finance of China (MOF) and administrated by the Chinese Academy of Sciences CAS.

## References

- Fu, L., Wang, Y.-F., & Qian, H.-L. 2019, *Progress in Astronomy*, 37, 187 (in Chinese)
- Gawronski, W. 2004, *IEEE Antennas and Propagation Magazine*, 46, 50
- Gu, L.-B., & Zhao, X.-R. 2017, *Fire Control Radar Technology*, 46, 80 (in Chinese)
- He, G.-L., Li, G.-M., Liu, M., & Huang, Y. 2009, *International Workshop on Intelligent Systems and Applications*, Wuhan, 1
- He, F.-L., Xu, Q., Wang, N., et al. 2020, *RAA (Research in Astronomy and Astrophysics)*, 20, 199
- Huang, L., Ma, W.-L., & Huang, J.-L. 2016, *New Astronomy*, 47, 105
- Leng, G.-J., Wang, W., Duan, B.-Y., & Li, X.-P. 2011, *System Engineering and Electronics*, 33, 996 (in Chinese)
- Liu, B.-H., Cheng, C.-H., & Yuan, H.-P. 2019, *Electro-Mechanical Engineering*, 35, 5 (in Chinese)
- Subrahmanyam, R. 2005, *IEEE Transactions on Automatic Control*, 53, 2590
- Wang, N. 2014, *SCIENTIA SINICA Physica, Mechanica & Astronomica*, 44, 783
- Wang, C.-S., Xiao, L., Wang, W., et al. 2017, *RAA (Research in Astronomy and Astrophysics)*, 17, 43
- Yu, C.-Y., & Fan, X.-H. 2019, *Equipment Environmental Engineering*, 16, 90 (in Chinese)
- Zhang, J., Lei, Z.-G., Quan, Z.-J., et al. 2015, *Fifth Asia International Symposium on Mechatronics (AISM 2015)*, Guilin, 1
- Zhang, J., Huang, J., Zhou, J., Wang, C.-S., & Zhu, Y. 2016, *IEEE Transactions on Control Systems Technology*, 5, 1
- Zhang, D.-D., Bao, H., Wei, S.-T., & Xu, Q. 2018, *Electro-Mechanical Engineering*, 34, 60 (in Chinese)
- Zhang, J., Huang, J., Liang, W., et al. 2018, *Shock and Vibration*, 2018, 3262869